Available online at www.sciencedirect.com
SCIENCE DIRECT®
Journal of Solid State Chemistry 178 (2005) 2663–2672
JOURNAL OF SOLID STATE CHEMISTRY
www.elsevier.com/locate/jssc

IRRS, UV-Vis-NIR absorption and photoluminescence upconversion in Ho^{3+}-doped oxyfluorophosphate glasses

Basudeb Karmakar*

Glass Division, Central Glass and Ceramic Research Institute, 196 Raja S.C. Mullick Road, Kolkata 700 032, India

Received 15 April 2005; received in revised form 2 June 2005; accepted 13 June 2005
Available online 19 July 2005

Abstract

Infrared reflection spectroscopic (IRRS), ultraviolet-visible-near infrared (UV-Vis-NIR) absorption and photoluminescence upconversion properties with special emphasis on the spectrochemistry of the oxyfluorophosphate (oxide incorporated fluorophosphates) glasses of the $Ba(PO_3)_2$–AlF_3–CaF_2–SrF_2–MgF_2–Ho_2O_3 system have been studied with different concentrations (0.1, 0.3 and 1.0 mol%) of Ho_2O_3. IRRS spectral band position and intensity of Ho^{3+} ion doped oxyfluorophosphate glasses have been discussed in terms of reduced mass and force constant. UV-Vis-NIR absorption band position has been justified with quantitative calculation of nephelauxetic parameter and covalent bonding characteristics of the host. NIR to visible upconversion has been investigated by exciting at 892 nm at room temperature. Three upconverted bands originated from the $^5F_3 \rightarrow {}^5I_8$, ($^5S_2$, $^5F_4$)$\rightarrow {}^5I_8$ and $^5F_5 \rightarrow {}^5I_8$ transitions have found to be centered at 491 nm (blue, medium), 543 nm (green, very strong) and 658 nm (red, weak), respectively. These bands have been justified from the evaluation of the absorption, normal (down conversion) fluorescence and excitation spectra. The upconversion processes have been explained by the excited state absorption (ESA), energy transfer (ET) and cross relaxation (CR) mechanisms involving population of the metastable (storage) energy levels by multiphonon deexcitation effect. It is evident from the IRRS study that the upconversion phenomena are expedited by the low multiphonon relaxation rate in oxyfluorophosphate glasses owing to their high intense low phonon energy ($\sim$600 cm^{-1}) which is very close to that of fluoride glasses (500–600 cm^{-1}).

Keywords: IRRS; Isosbestic point; UV-Vis-NIR; Nephelauxetic effect; Electronegativity; Covalent bonding; Upconversion; Holmium; Fluorophosphate glass

1. Introduction

Photoluminescence upconversion is a process in which photons of lower energy excitation light (NIR) are converted within the optical materials into the photons of higher energy emission light (visible). According to the energy conservation principle, it requires at least two photons to work simultaneously irrespective of the category of mechanisms. Bloembergen [1] was the first to observe the upconversion phenomenon in a rare earth (RE) ion doped crystal in 1959, and Auzel [2] was the first to review and explore it in 1973. Currently, there is a renewed interest in this group of solid-state laser materials to develop compact visible lasers seeking to either enhance the efficiencies of the existing devices or to create new ones. The principal uses of upconversion lasers are in optical data storage, bar-code reading, laser printing, submarine communication, biomedical instrument and spectroscopic applications [3–5]. The trivalent holmium ion (Ho^{3+}) is one of the most important active ions in the RE family (cerium to lutetium) due to its convenient energy level structure (Fig. 1) exploitable in upconversion processes. Within the Ho^{3+} ion energy scheme tricolor visible upconversion processes can take place from the $^5F_3 \rightarrow {}^5I_8$ (blue), $^5S_2 \rightarrow {}^5I_8$ (green) and $^5F_5 \rightarrow {}^5I_8$ (red) transitions. The efficiency of these emissions are strongly dependent on the characteristics of the glass host which determine a variety of parameters such as multiphonon

*Fax: +91 33 2473 0957.
E-mail address: basudebk@cgcri.res.in.

0022-4596/$ - see front matter © 2005 Elsevier Inc. All rights reserved.
doi:10.1016/j.jssc.2005.06.007

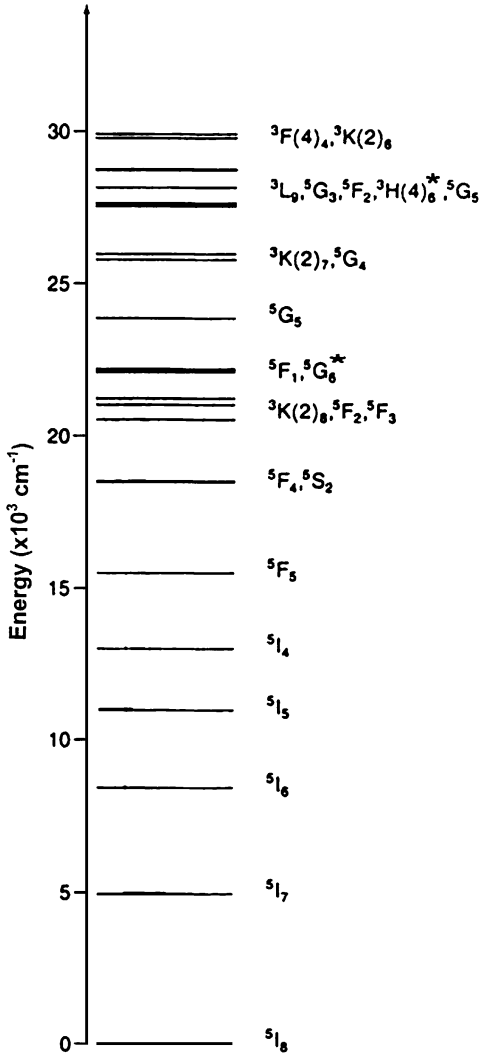

Fig. 1. Schematic energy level diagram of Ho^{3+} ion.

decay rates, population of metastable (storage) energy levels, energy transfer (ET) and cross relaxation (CR) rates decided by resonances in the energy level structure and also by the active ion concentration.

In phosphate glasses, the upconversion phenomenon is very faint, because of the large multiphonon decay rates, due to high energy stretching vibration of the P–O bond, that is, high phonon energy ($\sim$1300 cm^{-1}) [6–8]. However, their phonon energy can be reduced down to $\sim$600 cm^{-1} [6,9,10] by incorporating metal fluorides because of their low phonon energy (200–400 cm^{-1}) [11]. The low phonon energy of the fluorophosphate glasses yields low nonradiative decay and high radiative emission rates of RE ion energy levels, leading to much higher quantum efficiencies than the phosphate glass hosts but similar to that of fluoride glasses having comparable phonon energy 500–600 cm^{-1} [11], for transitions departing from levels with small energy gaps to the next lower laying levels [11,12]. These characteristics of fluorophosphate glasses make them more preferable than fluoride glasses because of their following technological advantages [10,13]: easy to prepare in open atmosphere (no need of expensive glove box), no serious chemical corrosion of the crucible and comparatively low tendency to crystallize due to high value of $T_x - T_g$ (an indicator of thermal stability of a glass, where T_x and T_g are the onset of crystallization and glass transformation temperatures, respectively). However, the presence of phosphate deteriorates some optical properties of the glasses. In order to obtain a glass with optimum optical properties, the phosphate content should be kept as low as practicable.

Although several papers have been published reporting the spectroscopic properties of fluoro- and chlorophosphate glasses doped with Ho^{3+} ions [14,15], the understanding of their spectrochemistry is rather very insufficient. However, to the best of our knowledge, there is no report dealing with the upconversion fluorescence characteristics of Ho^{3+}-doped oxyfluorophosphate (oxide incorporated fluorophosphate) glasses along with their IRRS spectral study.

Pondering with these issues, in this paper we aim to report a germane study on the IRRS, UV-Vis-NIR absorption and photoluminescence upconversion properties with special emphasis on the spectrochemistry of Ho^{3+} ion doped oxyfluorophosphate glasses.

2. Experimental

The base glass of the composition (mol%) $7Ba(PO_3)_2 \cdot 32AlF_3 \cdot 30CaF_2 \cdot 18SrF_2 \cdot 13MgF_2$ was prepared by melting 100 g batch using analytical grade $Ba(PO_3)_2$, AlF_3, CaF_2, SrF_2 and MgF_2 in a covered platinum crucible at 1020 °C for 1 h in air. The melt was cast into a hot graphite mould and properly annealed. This base glass was ground and doped with 0.1, 0.3 and 1.0 mol% Ho_2O_3 (99.99%, Alfa Aesar) and melted in a similar procedure. After cutting, grinding and/or polishing, they were used for characterization.

The density of the glasses was measured by the Archimedes method using water. The thermal properties were measured by a dilatometer (Netzsch, DIL 402C) at the heating rate of 5 K/min in air. The refractive indices at various wavelengths were measured (error limit: $\pm$0.0002) with a refractometer (Pulfrich, PR 2). The infrared reflection spectra (IRRS) in the range 400–1500 cm^{-1} were recorded with a Fourier transform infrared (FTIR) spectrometer (Perkin-Elmer, FTIR 1615) at an incident angle of 15° with the help of a specular reflectance measurement accessory at the resolution of $\pm 2\,cm^{-1}$ and after 100 scans. The absorption spectrum in the range 4000–6000 cm^{-1} was also measured in the absorption mode using this FTIR spectrometer at the same precision. The instrument was calibrated with the peaks of a standard polystyrene film

supplied by the manufacturer of the instrument. The UV-Vis-NIR absorption spectrum in the range 300–1000 nm was obtained with a double-beam spectrophotometer (Perkin-Elmer, Lambda 20) keeping the base glass of the same thickness in the reference beam. The instrument was calibrated with the peaks of a standard holmium ion (Ho^{3+})-doped glass filter supplied by the manufacturer of the instrument and the validity of the peak position was found to be ± 0.1 nm. Fluorescence spectra were measured, at the accuracy of ± 0.2 nm, with a fluorescence spectrophotometer (Spex, Fluorolog 2) in which a Xenon lamp is attached as a monochromated excitation source and a photomultiplier tube (PMT) as a detector. All the measurements were carried out at room temperature.

3. Results

3.1. Physical properties

Values of important glass properties such as density (d), transformation (T_g) and deformation (T_d) temperatures, coefficient of thermal expansion (α_{CTE}) and refractive indices (n_i) at various wavelengths of 0.1 mol% Ho_2O_3-doped oxyfluorophosphate glass estimated by the relevant standard methods are given in Table 1. Various other physical properties like Ho^{3+} ion number concentration (N), average molecular weight (M_{av}), molar volume (V_m) and refractivity (M_R), reflection loss (R), inter-ionic distance (r_i) of Ho^{3+} ions, polaron radius (r_p), molecular electronic polarizability (α) of the glass, etc., have been evaluated based on the composition, density and refractive index of the glass using the established expressions available in the literature [16–18]. These values are also listed in Table 1. All the properties exhibit the optical efficiencies of the glass under investigation.

Table 1
Measured and calculated physical properties of 0.1 mol% Ho_2O_3-doped oxyfluorophosphate glass

Physical property	Value
Measured property	
Density, d ($g\,cm^{-3}$)	3.56
Transformation temperature, T_g (°C)	439
Deformation temperature, T_d (°C)	473
Coefficient of thermal expansion, α_{CTE} ($°C^{-1}$) (30–300 °C)	163×10^{-7}
Refractive index	
n_d (at $\lambda = 587.1$ nm)	1.4594
n_e (at $\lambda = 546.1$ nm)	1.4606
$n_{C'}$ (at $\lambda = 643.8$ nm)	1.4580
Calculated property	
Ho^{3+} ion concentration, N ($ions\,cm^{-3}$)	4.22×10^{19}
Average molecular weight, M_{av}	101.69
Molar volume, V_m (cm^3)	28.56
Molar refractivity, M_R (cm^3)	7.81
Reflectivity per surface, R (%)	3.49
Dielectric constant, ε	2.1298
Polaron radius, r_p (Å)	11.58
Inter-ionic distance, r_i (Å)	28.72
Field strength, F (cm^{-2})	4.823×10^{-17}
Molecular electronic polarizability factor, α (cm^3)	1.547×10^{-21}

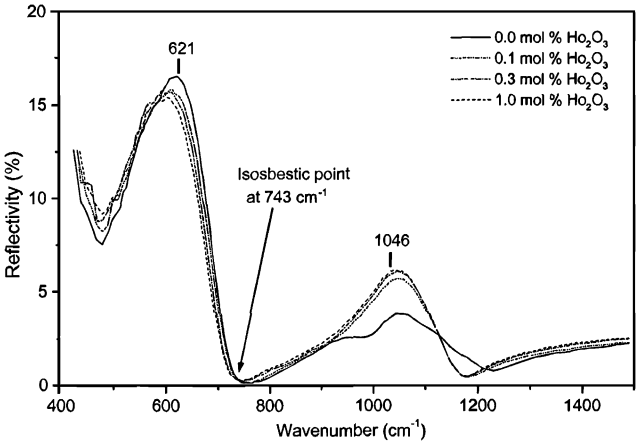

Fig. 2. IRRS spectra of as-polished undoped and Ho_2O_3-doped oxyfluorophosphate glasses at an incident angle of 15°.

3.2. IRRS spectra

Infrared reflection spectroscopic (IRRS) spectra in the range 400–1500 cm^{-1} of undoped and Ho^{3+} ion doped oxyfluorophosphate glasses are shown in Fig. 2. There are three major reflection bands in the undoped glass centered at about 1046, 940 and 621 cm^{-1}. Whereas all the Ho^{3+} ion doped glasses have only two bands centered at about 1046 and 621 cm^{-1}. Fig. 3 further shows that as the Ho^{3+} ion concentration increases, the 1046 cm^{-1} band shifts towards higher frequency and its reflectivity (intensity) increases. While Fig. 4 shows that the 621 cm^{-1} band position shifts towards lower frequency and its reflectivity (intensity) decreases with increasing in Ho^{3+} ion concentration. As a consequence of intensity increase in the band at ~1046 cm^{-1} and decrease in the band at ~621 cm^{-1}, all the curves cross at 743 cm^{-1} (Fig. 2). This crossing point is known as the isosbestic point which represents the existence of an equilibrium between two IR reflecting species.

3.3. UV-Vis-NIR absorption spectra

The ultraviolet-visible-near infrared (UV-Vis-NIR) absorption spectra are shown in Fig. 5. A total of 11 absorption bands from the ground state $^5I_8$ of Ho^{3+} ion have been observed. Their associated transitions in comparison with those in fluoride glass (ZBLANP) [19] and aqueous solution [20] are provided in Table 2 to correlate band position with the nephelauxetic

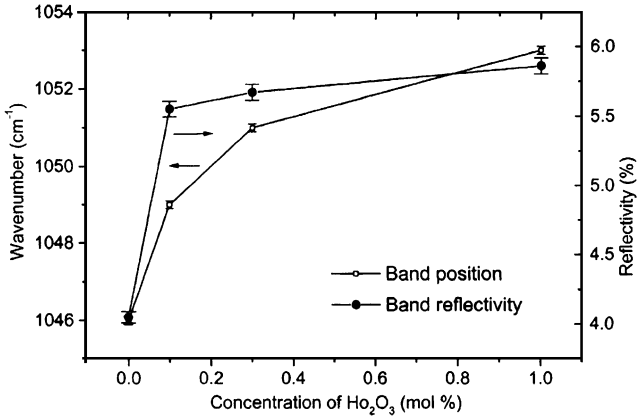

Fig. 3. Band position and reflectivity at ~1046 cm^{-1} as a function of Ho_2O_3 concentration in oxyfluorophosphate glasses.

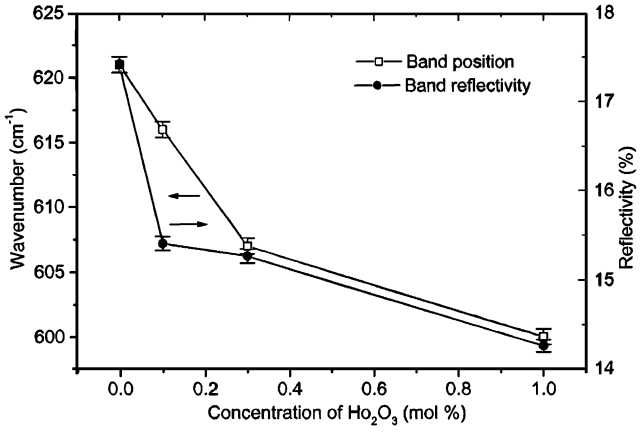

Fig. 4. Band position and reflectivity at ~621 cm^{-1} as a function of Ho_2O_3 concentration in oxyfluorophosphate glasses.

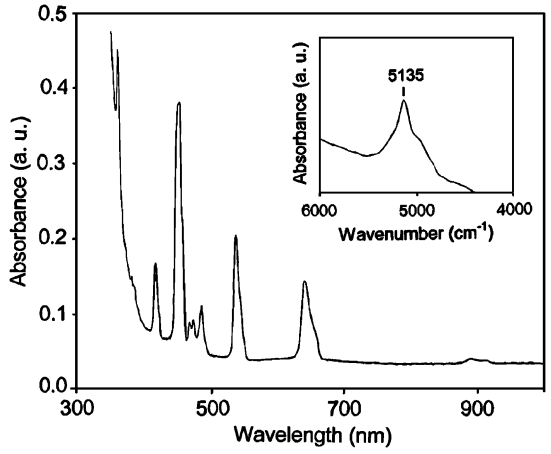

Fig. 5. Ground state absorption (GSA) spectra of the 0.1 mol% Ho_2O_3-doped oxyfluorophosphate glass in the ranges of 300–1000 nm and 4000–6000 cm^{-1} (inset). The assignments of the bands are given in Table 2.

parameter and bonding characteristics of the hosts (see Section 4.2). The increasing order of intensity of the bands: $^5I_7 < {}^5I_5 < {}^3K_8 < {}^5F_2 < {}^5F_3 < {}^5F_5 \approx {}^5G_4$, $^3K_7 < {}^5G_5 < {}^5S_2$, $^5F_4 < {}^5G_6$, $^5F_1 < {}^3H_5$, $^3H_6$. It is worth noting that the high intensity bands are located at 359.6 and 450.6 nm originated from the $^5I_8 \rightarrow {}^3H_6$ and $^5I_8 \rightarrow {}^5G_6$ transitions, respectively. It has happened due to their hypersensitive pseudoquadrupole transition characteristics, in Fig. 1 they are marked by asterisk, obeying the selection rules $|\Delta J| \leqslant 2$, $|\Delta L| \leqslant 2$ and $\Delta S = 0$, where J, L and S are the total angular momentum, orbital quantum number and spin quantum number, respectively [21]. These transitions are hypersensitive with large values of the reduced matrix element, $\langle U^{(2)} \rangle^2$ (0.2155 and 1.5201 for the $^5I_8 \rightarrow {}^3H_6$ and $^5I_8 \rightarrow {}^5G_6$ transitions, respectively [20]) of the Judd–Ofelt tensor. Their line strength then becomes hypersensitive to the Judd–Ofelt parameter Ω_2 (a parameter commonly used as an indicator of the type of bonding with the RE ions in the host).

3.4. Photoluminescence upconversion

The upconversion emission spectra of 0.1, 0.3 and 1.0 mol% Ho_2O_3-doped oxyfluorophosphate glasses are shown in Fig. 6. Three upconverted bands are observed to be centered at 491 nm (blue, medium), 543 nm (green, very strong) and 658 nm (red, weak) originated from the $^5F_3 \rightarrow {}^5I_8$, ($^5S_2$, $^5F_4$) $\rightarrow {}^5I_8$ and $^5F_5 \rightarrow {}^5I_8$ transitions. The intensity variation of these bands with concentration of Ho_2O_3 is shown in Fig. 7. Similar tricolor emission bands (not shown here) and trend of variation of their intensity with concentration of Ho_2O_3 (Fig. 8) are also observed in normal (down conversion) fluorescence spectra on excitation of the hypersensitive band at 451 nm. Excitation spectrum with emission at 543 nm (the strongest green up and down conversion emission band) is shown in Fig. 9. Both the absorption (Fig. 5) and excitation (Fig. 9) spectra clearly advocate the normal fluorescence which in turn supports the origin of the above shown upconverted bands (Fig. 6). This upconverted behavior of Ho^{3+} ion in the oxyfluorophosphate glasses conforms well to those observed in fluoride hosts such as ZBLAN glasses [22,23] and $LiYF_4$ crystals [22,24].

4. Discussion

4.1. Interpretation of IRRS spectra

The bands as shown in Fig. 2 have been assigned based on our previous work [6–8] as follows: 1046 cm^{-1} band to the stretching vibration of the P–O^- bonds of $[PO_4]^{3-}$ ions, 940 cm^{-1} band to the stretching vibration of fluorophosphates units [25,26] and 621 cm^{-1} band to the asymmetric stretching vibration of bridging fluorine atoms in the octahedrally coordinated Al–F–Al groups of the mixture of oxyfluoro- and fluoro-species such as

Table 2
UV-Vis-NIR absorption bands and their associated transitions of Ho^{3+} ion doped oxyfluorophosphate glass

Transitions		Band position			
Ground state	Excited state	Oxyfluorophosphate glass (this study)		ZBLANP fluoride glass[a] [19] (cm^{-1})	Aqueous solution[a] [20] (cm^{-1})
		±0.1 (nm)	±2 (cm^{-1})		
$^5I_8 \rightarrow$	$^5I_7$	1947.4	5135	5140	5130
	$^5I_5$	891.5	11,217	11,250	11,120
	$^5F_5$	640.5	15,612	15,649	15,500
	$^5S_2$, $^5F_4$	536.2	18,649	18,690	18,500
	$^5F_3$	484.5	20,639	20,700	20,600
	$^5F_2$	472.5	21,164	—	21,100
	$^3K_8$	466.6	21,431	21,460	21,370
	$^5G_6$, $^5F_1$	450.6	22,192	22,320	22,100
	$^5G_5$	416.2	24,026	24,100	23,950
	$^5G_4$, $^3K_7$	383.1	26,102	—	25,800
	$^3H_5$, $^3H_6$	359.6	27,808	27,860	27,700

[a]Band positions of Ho^{3+} ion in fluoride glass and aqueous solution are given for comparison.

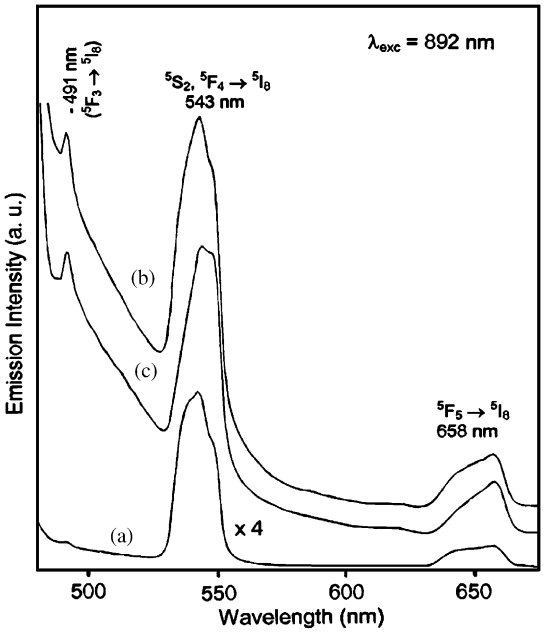

Fig. 6. Upconversion fluorescence spectra of: (a) 0.1, (b) 0.3, and (c) 1.0 mol% Ho_2O_3-doped oxyfluorophosphate glasses upon excitation at $\lambda_{exc} = 892$ nm. (The bases of the curves b and c are lifted for better visualization.)

$F_3Al–O–AlF_3$ and $[AlF_6]^{3-}$. The strongly charged Al^{3+} ion links two or more fluorophosphate tetrahedral $[PO_2F_2]^{3-}$ or $[PO_3F]^{2-}$ ions [27,28] to make the polymeric glass matrix. On incorporation of Ho_2O_3 in fluorophosphate glasses, the Ho^{3+} ion brings about the breaking of these bridges and enters into the fluoride phase as a result of the following type of reactions:

$$3[PO_2F_2]^{3-}_{\text{Tetrahedra}} + [HoO_3]^{3-}_{\text{Octahedra}} + 3[Al_2F_6O]_{\text{Octahedra}} = 3[PO_4]^{3-}_{\text{Tetrahedra}} + [HoF_6]^{3-}_{\text{Octahedra}} + 3[Al_2F_6]_{\text{Planar-bridge}}. \quad (1)$$

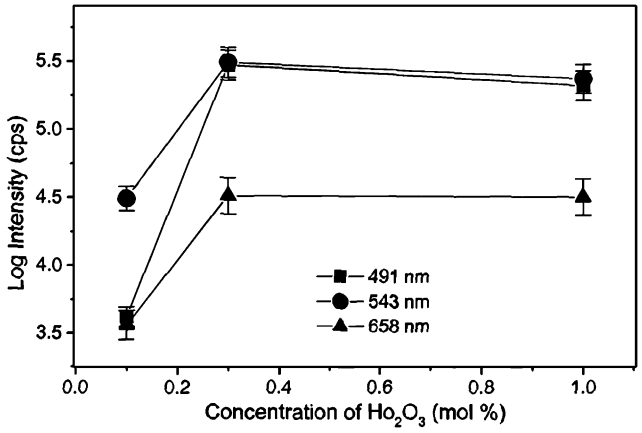

Fig. 7. Ho_2O_3 concentration dependence of intensity of upconversion fluorescence bands at 491, 543, and 658 nm upon excitation at $\lambda_{exc} = 892$ nm.

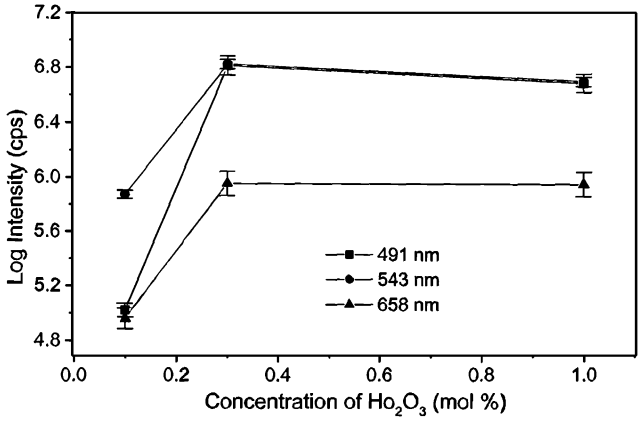

Fig. 8. Ho_2O_3 concentration dependence of intensity of normal (down conversion) fluorescence bands at 491, 543, and 658 nm upon excitation at $\lambda_{exc} = 451$ nm.

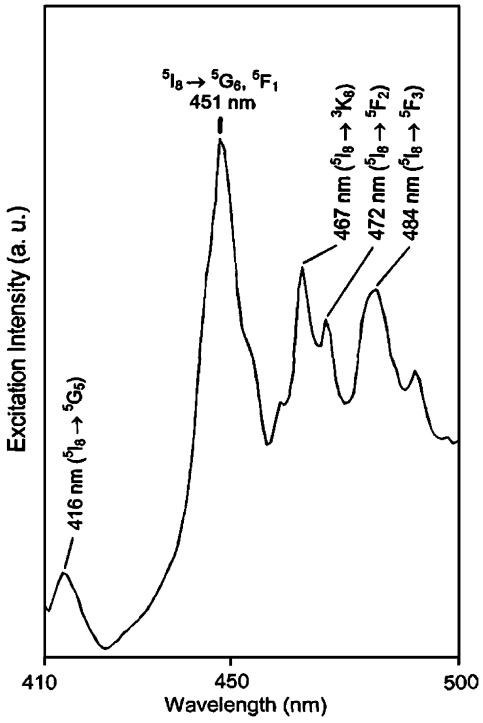

Fig. 9. Excitation spectrum with emission at $\lambda_{emi} = 543$ nm (the strongest green up and down conversion emission band) of the 0.1 mol% Ho_2O_3-doped oxyfluorophosphate glass.

Consequently, the concentration of the phosphate species gradually increases and likewise the intensity of the 1046 cm^{-1} band. The disappearance of the band at 940 cm^{-1} confirms that it must be due to a fluorophosphates group and support the above reaction [26].

The shifting of the band position can be illustrated by the Szigeti relation [29] of fundamental vibration frequency, v (in cm^{-1}) as follows:

$$v = (k/4\pi^2 c^2 \mu)^{0.5} \quad (2)$$

which stipulates that the position of the fundamental phonon frequency, ω (wavenumber) is related to the force constant (k), reduced mass (μ) and speed of light (c). The μ can be defined by

$$\mu = m_1^{-1} + m_2^{-1}, \quad (3)$$

where m_1 and m_2 are the masses of the bond forming two atoms. It is, therefore, obvious from Eqs. (2) and (3) that the v of the fluoride species at 621 cm^{-1} decreases with increasing μ due to incorporation of heavier Ho^{3+} ions into the fluoride phase. Considering the reaction as shown in Eq. (1), similar arguments can be imposed for the shifting of the phosphate band at 1046 cm^{-1} towards higher frequency as well as its intensity increase.

It is well known that the intensity of an IR band is directly controlled by the dipole moment (μ_{DM}) gradient, $\delta\mu_{DM}/\delta r$ [6,27] and indirectly by the force constant (k). The k (in mdyn $Å^{-1}$) may be expressed as [30]:

$$k = 1.67\, N(\chi_1\chi_2/r^2)^{0.75} + 0.3, \quad (4)$$

where N is the bond order, χ_1 and χ_2 are the electronegativities of the atoms, and r is the bond distance. The changes in μ_{DM}, r, k, etc., which have happened due to incorporation of Ho_2O_3 in the glass matrix are, thus, responsible for increase and decrease in intensity of the bands at 1046 and 621 cm^{-1}, respectively [6,27,31]. As a consequence of this fact, the IRRS curves show an isosbestic point at 743 cm^{-1} (Fig. 2). The observation of the isosbestic point is a good evidence of the presence of phosphate and fluoride as two principal species. It is also a strong argument in favor of the existence of equilibrium between them in the oxyfluorophosphate glasses in presence of Ho^{3+} ions [32].

4.2. Quantitative justification of UV-Vis-NIR absorption band position

From inspection of the comparative UV-Vis-NIR absorption positions of Ho^{3+} ions in various hosts as listed in Table 2, it is seen that the bands of the oxyfluorophosphate glass belong to in between position of the fluoride glass and the aqueous solution. Here the aqueous solution has been considered because of property-wise it is very close to that of $Ba(PO_3)_2$ glass (see Table 3) [33]. Thus, the band position shifts towards lower frequency (energy) with the order of host: ZBLANP fluoride glass < oxyfluorophosphate glass < aqueous solution. This shift can be interpreted in terms of chemical bonding property of the ligand (here fluorine or oxygen) that exerts influences on the position of the absorption bands due to the so-called *''nephelauxetic effect''* (literally means ''charge cloud expansion''). Here, it may be noted that the nephelauxetic shift is largely more discernible for those transitions in which the electric dipole–dipole type interaction dominates. According to Jørgensen [34], owing to this effect, the phenomenological parameters of interelectron repulsion are smaller in a host than in the corresponding free ions. Mathematically, the Hamiltonian operator (H_{fi}) of a free paramagnetic ion can be expressed as [35]:

$$H_{fi} = H_{el} + H_{so} + H_{cf}, \quad (5)$$

where H_{el} is the electrostatic interaction of the electron, H_{so} is the spin–orbit interaction, and H_{cf} is the interaction of the electrons with the crystal field due to environment. When an ion is incorporated into a host, due to nephelauxetic effect, the parameters H_{el}, H_{so} and H_{cf} are reduced from their free ion values. All these causes a contraction of the energy level structure of the ion in that particular host compared to that of free ion. Consequently, this leads to a shift of the absorption bands towards lower frequency. Quantitatively, this fact can be expressed by the nephelauxetic

Table 3
Nephelauxetic parameter, electronegativity, covalent and ionic bonding characteristics of various host of Ho^{3+} ion

Host of Ho^{3+} ion	Composition (mol%)	Nephelauxetic parameter, β ($\times 10^{-2}$)	Electronegativity, $\Delta\chi$	Covalent character (%)
ZBLANP fluoride glass	51.5 ZrF_4–19.5 BaF_2–5.3 LaF_3–3.2 AlF_3–18.0 NaF–2.5 PbF_2	1.87	2.8	14
Oxyfluoro-phosphate glass	7 $Ba(PO_3)_2$–32 AlF_3–30 CaF_2–18 SrF_2–13 MgF_2	2.05	2.6	18
Aqueous solution	100 H_2O	2.43	1.4	61
Barium metaphosphate glass[a]	100 $Ba(PO_3)_2$	—	1.8	56

[a]Corresponding values of barium metaphosphate glass are given for comparison with those of aqueous solution.

parameter, β as [34]:

$$\beta = (\sigma_{fi} - \sigma_{ih})/\sigma_{fi}, \quad (6)$$

where σ_{fi} and σ_{ih} are the maximum absorption frequency of the free ion and the ion in a given host, respectively. The calculated values of β obtained using Eq. (6) and $\sigma_{fi} = 28,391\,cm^{-1}$ [36] for the hypersensitive $^5I_8 \rightarrow {}^3H_6$ transition have been listed in Table 3. The nephelauxetic effect is explained by Jørgensen as an expansion of the partly filled shell ($4f^{n-1}$ of RE ions) due to the transfer of the ligands to the core of the central RE ion. It is, therefore, a measure of covalency effect [33,37]. The degree of covalent bonding character of a host can be estimated approximately using the formula [38]:

$$\text{Covalent character (\%)} = \exp[-0.25(\Delta\chi)^2] \times 100, \quad (7)$$

where $\Delta\chi$ is the electronegativity of the glass, that is, the electronegativity difference (χ_A–χ_C) of the anions and the cations. The average electronegativity of anions (χ_A) or cations (χ_C) can be evaluated by the following simple additive relation [5]:

$$\chi_A \text{ or } \chi_C = \sum N_i\chi_i / \sum N_i, \quad (8)$$

where N_i and χ_i are the number of individual constituent atom per mole and its electronegativity, respectively.

The calculated values of electronegativity, covalent and ionic bonding characteristics of various hosts of the Ho^{3+} ion obtained using Eqs. (7) and (8) are also provided in Table 3. In this calculation Pauling's electronegativity values [38] were used. All the calculated values of aqueous solution agree well with those of Pauling [38] which advocates the above calculation method and the data obtained thereof for glasses. It is obvious from the data presented in Table 3 that the nephelauxetic parameter increases with increasing in covalent character but decreasing in electronegativity and ionic character. It, therefore, clearly indicates the existence of a reliable correlation between the nephelauxetic parameter and the covalent bonding characteristics of various hosts of the Ho^{3+} ion. Hence, the increasing order of the nephelauxetic parameter or covalent bonding character of host is: ZBLANP fluoride glass < oxyfluorophosphate glass < aqueous solution. This is analogous to the sequence of shifting of the absorption band positions of Ho^{3+} ion found in these hosts as mentioned earlier (and also see Table 2).

4.3. Interpretation and mechanism of photoluminescence upconversion

The oxyfluorophosphate glasses doped with different concentrations of Ho_2O_3 (0.1, 0.3 and 1.0 mol%) under excitation at 892 nm emit three upconverted fluorescence bands centered at 491, 543 and 658 nm (Fig. 6) corresponding to the $^5F_3 \rightarrow {}^5I_8$, ($^5S_2$, $^5F_4$) $\rightarrow {}^5I_8$ and $^5F_5 \rightarrow {}^5I_8$ transitions, respectively. Similar emission bands have also been obtained in normal (down conversion) fluorescence spectra on excitation at 451 nm. A combination of three mechanisms such as excited state absorption (ESA), ET and CR as shown in Fig. 10 and described below can explain the observed upconversion emissions [22–24,39–41].

(i) *ESA*: The fluorescence band intensity increasing order is red band (658 nm) < blue band (491 nm) < green band (543 nm). This order remains constant irrespective of the concentration of Ho_2O_3, up and down conversions (Table 4 and Figs. 7 and 8). From inspection of the ratio of I_{491}:I_{543}:I_{658} both of up and down conversions for different concentrations of Ho_2O_3 (Table 4), it is seen that the highest ratio exhibits in the lowest concentration of Ho_2O_3. It suggests that at low concentration, the dominant mechanism is the ESA, which means the ET process can generally be neglected. Because of the efficiency of ESA is independent of Ho^{3+} ion concentration since it involves only one active ion. In the ESA process, the absorption of the first pump photon (892 nm) by a Ho^{3+} ion (GSA), a population will grow in the $^5I_5$ energy level of the same ion which will increase the possibility of absorbing another pump photon by exciting it to the $^5G_6$, $^5F_1$ levels (ESA) in the order: $^5I_8 \rightarrow {}^5I_5 \rightarrow {}^5G_6$, $^5F_1$. Because of the

manifolds $^5G_6$, $^5F_1$ have energy corresponding to two 892 nm photons.

The difference in the intensity of the blue, green and red fluorescence bands has happened due to the difference in population of the $^5F_3$, $^5S_2$ and $^5F_5$ metastable energy levels. The highest intensity of the green band at 543 nm is caused by the highest population of the $^5S_2$ level supervened by the nonradiative multiphonon relaxation process through $^5F_3$– $^5S_2$ because of the higher energy gap of ΔE ($^5G_6$– $^5S_2$) than ΔE ($^5G_6$– $^5F_3$). The rate of multiphonon relaxation process (k_{MP}) may be expressed as [12]:

$$k_{MP} = \beta e^{-\alpha p}, \quad (9)$$

where α and β are two host-dependent constants, and p is the phonon order. The value of p can be calculated using the relation:

$$p = \Delta E/\hbar\omega, \quad (10)$$

where ΔE is the energy gap (3543 cm^{-1}) between $^5G_6$ and $^5S_2$ levels, and $\hbar\omega$ is the phonon energy of the glass host. From IRRS spectra (Fig. 2), $\hbar\omega$ is found to be about 600 cm^{-1}. It gives a value of about 6 to p which involved in this relaxation process. The k_{MP} decreases strongly with increasing in p according to Eq. (9). It is reported that low $\hbar\omega$ of the host can be obtained from the phonon side band (PSB) spectra than that of the IRRS spectra [42]. Because of the vibration of PSB originates from the local vibration around the RE ions only whereas in IRRS that represents the total vibrations of the whole matrix [43]. However, the average $\hbar\omega$ values of fluoride glasses obtained by PSB spectra have been found to be very close to those obtained from the low frequency stretching vibrations of IRRS spectra [11,42–44]. It should be noted here that the dominant $\hbar\omega$ would be 1046 cm^{-1} for the glasses with higher phosphate content. This is because of the fact that the electron–phonon coupling strength increased greatly with increasing phosphate [45].

In the above way, the population of $^5F_5$ metastable energy level is low due to very large (3037 cm^{-1}) energy gap, ΔE ($^5S_2$– $^5F_5$). The alternative way of population of the $^5F_5$ level is as follows. Close examination of the energy level structure of Ho^{3+} ion for the 892 nm pump photon (Fig. 10) discloses a quasi-resonant ESA transition of $^5I_7 \rightarrow {}^5F_5$. The intermediate $^5I_7$ level is a long-lived one and populated by the multiphonon decay process of $^5I_5 \rightarrow {}^5I_6 \rightarrow {}^5I_7$, owing to low phonon energy (~600 cm^{-1}) of oxyfluorophosphate glasses because of the large energy (5135 cm^{-1}) gap, ΔE ($^5I_7$– $^5I_8$). In this condition, ESA transition $^5I_7 \rightarrow {}^5F_5$ dominates the red emission transition of $^5F_5 \rightarrow {}^5I_8$ at 658 nm. Since the pumping wavelength 892 nm is not exactly resonant with this ESA transition, so the weak intensity of the red

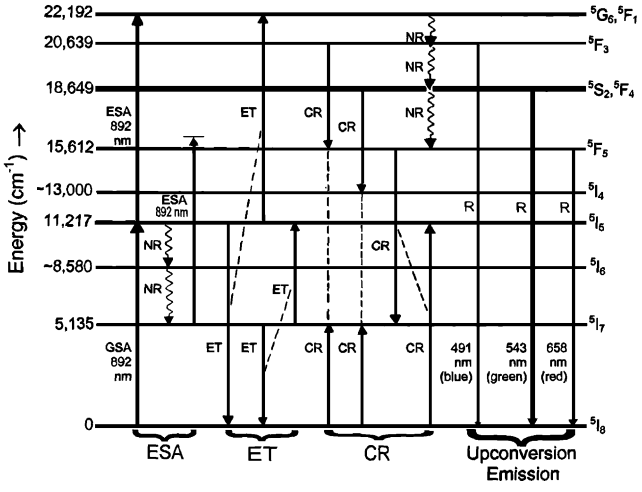

Fig. 10. Partial energy level diagram of the Ho^{3+} ion in oxyfluorophosphate glass showing transitions in GSA, ESA, ET, CR, and upconversion fluorescence emissions under $\lambda_{exc} = 892$ nm excitation (R and NR represent the radiative and nonradiative transitions, respectively).

Table 4
Variation in relative intensity of up and down conversion fluorescence bands at 491 nm (I_{491}), 543 nm (I_{543}) and 658 nm (I_{658}) with concentration of Ho_2O_3, inter-ionic distance and polaron radius

Topic	Corresponding values		
Concentration of Ho_2O_3 (mol%)	0.1	0.3	1.0
Inter-ionic distance, r_i (Å)	28.7	19.8	13.2
Polaron radius, r_p (Å)	11.6	8.0	5.3
Up conversion ($\lambda_{exc} = 892$ nm)			
Ratio of I_{491} at different concentration	1	70.5	56.1
Ratio of I_{543} at different concentration	1	10.0	6.8
Ratio of I_{658} at different concentration	1	9.1	8.7
Ratio of I_{491}:I_{543}:I_{658} at same concentration	1:7.40:0.86	1:1.05:0.11	1:0.90:0.13
Down conversion ($\lambda_{exc} = 451$ nm)			
Ratio of I_{491} at different concentration	1	60.8	45.4
Ratio of I_{543} at different concentration	1	8.8	6.5
Ratio of I_{658} at different concentration	1	10.0	9.7
Ratio of I_{491}:I_{543}:I_{658} at same concentration	1:7.09:0.86	1:1.03:0.14	1:0.90:0.18

band. This explanation agrees well with the ESA mechanisms proposed for fluoride glasses [22] and crystals [24].

(ii) *ET*: The intensity ratio data with respect to the blue emission band at 491 nm of up and down conversions with increasing concentration of Ho_2O_3 as listed in Table 4 reveal that the highest intensity of all the bands are at the concentration of 0.3 mol% Ho_2O_3. These are also depicted in the Figs. 7 and 8. This fact suggests the involvement of an ET process at relatively higher concentration of active ion. Since the ET process requires two Ho^{3+} ions in the intermediate excited states hence its efficiency depends on the Ho^{3+}–Ho^{3+} distance (r_i) or polaron radius (r_p), that is, on the concentration of Ho_2O_3. The r_i and r_p, for 0.3 mol% Ho_2O_3, are 19.8 and 8.0 Å, respectively (Table 4), which are near enough for the ET process to take place. The excited Ho^{3+} ions of the $^5I_5$ and $^5I_7$ levels transfer energy to another excited Ho^{3+} ion of these levels according to the resonant channels of ($^5I_5$, $^5I_5$)→($^5I_8$, $^5G_6$) and ($^5I_7$, $^5I_7$)→($^5I_8$, $^5I_5$), respectively. Such excitation of ET enhances by the low phonon energy of the oxyfluorophosphate glasses and results in higher population of $^5F_3$, $^5S_2$ and $^5F_5$ storage levels. The mechanism reported by Kishimoto et al. [41] corroborates the above ET processes.

(iii) *CR*: The intensity of all fluorescence bands decreases as the concentration of Ho_2O_3 increase beyond the 0.3 mol% (see Table 4 and Figs. 7 and 8). This is known as concentration quenching and occurs by the CR processes. Comparing the ionic radius (r) of Ho^{3+} ion ($r = 1.02-1.22$ Å in the coordination number (CN) range 8–12 [46]) with r_i (13.2 Å) and r_p (5.3 Å) for the 1.0 mol% Ho_2O_3 (Table 4), the CR processes appears to be responsible for decrease in intensity of the bands due to closer proximity of the Ho^{3+}–Ho^{3+} ion pair. It is observed that the concentration quenching of Sm^{3+} in various hosts due to CR starts when the mean distance of Sm^{3+}–Sm^{3+} approaches 12–15 Å [39]. In the present case, depopulation of the $^5F_3$, $^5S_2$ and $^5F_5$ storage levels enhances by the CR processes which begins with one Ho^{3+} ion in these excited levels and another one Ho^{3+} ion in the ground state ($^5I_8$). It occurs through the resonant channels of ($^5F_3$, $^5I_8$)→($^5F_5$, $^5I_7$), ($^5S_2$, $^5I_8$)→($^5I_4$, $^5I_7$) and ($^5F_5$, $^5I_8$)→($^5I_7$, $^5I_5$). It corresponds well with the CR processes in Ho^{3+}:$LiYF_4$ established by Kück and Sokólska [24]. The energy lost in the CR processes appears as lattice vibrations.

5. Conclusions

The major findings on the study of IRRS, UV-Vis-NIR absorption and photoluminescence upconversion properties of Ho^{3+}-doped oxyfluorophosphate glasses are as follows. Various physical properties of the 0.1 mol% Ho_2O_3-doped glass have been evaluated both experimentally and by theoretical calculation to establish its efficiency as an optical material. The variation of the IRRS spectral band position and reflectivity with different concentrations of Ho_2O_3 (0.1, 0.3 and 1.0 mol%) at ~1046 and ~621 cm^{-1} has been interpreted in terms of reduced mass and stretching force constant. The UV-Vis-NIR absorption band positions of Ho^{3+} ion have been justified by quantitative calculation of naphelauxetic parameter, electronegativity, and covalent bonding characteristics along with hosts. The photoluminescence upconversion bands centered at 491, 543 and 658 nm have been justified by the evaluation of the absorption, normal (down conversion) fluorescence and excitation spectra. The upconversion processes have been interpreted by the ESA, ET and CR mechanisms. IRRS spectra clearly reveal that the upconversion phenomenon is expedited by the low multiphonon relaxation rate in oxyfluorophosphate glasses owing to their low phonon energy (~600 cm^{-1}) which is very close to that of fluoride glasses (500–600 cm^{-1}). This study suggests that the Ho^{3+}:oxyfluorophosphate glasses may be considered as a potential candidate for applications in upconversion-based optical devices.

Acknowledgments

The author gratefully thanks Dr. H.S. Maiti, Director of the institute for his keen interest in this work and kind permission to publish this paper. He also wishes to thank Dr. K.K. Phani, Head, Glass Division for his kind support.

References

[1] N. Bloembergen, Phys. Rev. Lett. 2 (1959) 84.
[2] F.E. Auzel, Proc. IEEE 61 (1973) 758.
[3] W.P. Risk, T.R. Gosnell, A.V. Nurmikko, Compact Blue-Green Lasers, Cambridge University Press, Cambridge, 2003.
[4] G. Blasse, B.C. Grabmaier, Luminescent Materials, Springer, Berlin, 1994.
[5] B. Karmakar, R.N. Dwivedi, J. Non-Cryst. Solids 342 (2004) 132.
[6] B. Karmakar, P. Kundu, R.N. Dwivedi, J. Non-Cryst. Solids 289 (2001) 155.
[7] B. Karmakar, P. Kundu, R.N. Dwivedi, Mater. Lett. 57 (2002) 953.
[8] B. Karmakar, P. Kundu, R.N. Dwivedi, Mater. Lett. 47 (2001) 371.
[9] R. Ronchin, R. Rolli, M. Montagna, et al., J. Non-Cryst. Solids 284 (2001) 243.
[10] L.F. Santos, R.M. Almedia, V.K. Tikhomirov, A. Jha, J. Non-Cryst. Solids 284 (2001) 43.
[11] M.G. Drexhage, in: P.W. France, M.G. Drexhage, J.M. Parker, et al. (Eds.), Fluoride Glass Optical Fibres, Blackie, Glasgow, 1990, p. 1.
[12] S. Tanabe, J. Non-Cryst. Solids 256, 257 (1999) 282.
[13] A. Ozturk, J. Mater. Sci. 33 (1998) 73.

[14] A.V.R. Reddy, K. Annapurna, A.S. Jacob, S. Buddhudu, Ferrelectron. Lett. 15 (1993) 33.
[15] K. Naidu, S. Buddhudu, Mater. Lett. 14 (1992) 355.
[16] K. Annapurna, S. Buddhudu, J. Solid State Chem. 93 (1991) 454.
[17] G. Fluxy, G. Huang, S. Chen, J. Non-Cryst. Solids 52 (1982) 203.
[18] R. Harinath, S. Buddhudu, F.J. Bryant, L. Xi, Solid State Commun. 74 (1990) 1147.
[19] P.W. France, J. Non-Cryst. Solids 284 (2001) 132.
[20] W.T. Carnal, P.R. Fields, K. Rajnak, J. Chem. Phys. 49 (1968) 4424.
[21] R.D. Peacock, in: J.D. Dunitz, P. Hemmerich, R.H. Holm, et al. (Eds.), Structure and Bonding, vol. 22, Springer, Berlin, 1975, p. 83.
[22] A. Wnuk, M. Kaczkan, Z. Frukacz, et al., J. Alloys Compd. 341 (2002) 353.
[23] J.Y. Allain, M. Monerie, H. Poignant, Electron. Lett. 26 (1990) 261.
[24] S. Kück, I. Sokólska, Chem. Phys. Lett. 325 (2000) 257.
[25] H. Sun, L. Zhang, S. Xu, et al., J. Alloys Compd. 391 (2005) 151.
[26] I.A. Zhmyreva, V.P. Kolobkov, E.A. Lisitsyna, V.D. Khaliev, Sov. J. Glass Phys. Chem. 17 (1991) 55.
[27] B. Karmakar, P. Kundu, R.N. Dwivedi, J. Am. Ceram. Soc. 83 (2000) 1305.
[28] I.B. Urusovskya, E.V. Smirnova, S.A. Stepanov, Sov. J. Glass Phys. Chem. 17 (1991) 157.
[29] B. Szigeti, Proc. Soc. London Ser. A 204 (1950) 51.
[30] A.A. Higazy, B. Bridge, J. Mater. Sci. 20 (1985) 2345.
[31] B. Karmakar, P. Kundu, R.N. Dwivedi, Trans. Indian Ceram. Soc. 58 (1999) 19.
[32] E.D. Olsen, Modern Optical Methods of Analysis, McGraw-Hill, New York, 1975.
[33] R. Reisfeld, in: J.D. Dunitz, P. Hemmerich, J.A. Ibers, et al. (Eds.), Structure and Bonding, vol. 13, Springer, Berlin, 1973, p. 53.
[34] C.K. Jørgensen, Modern Aspects of Ligand Field Theory, North-Holland Publishing Co., Amsterdam, 1971.
[35] M.J. Weber, in: W.M. Yen, P.M. Selzer (Eds.), Laser Spectroscopy of Solids, Topics in Applied Physics, vol. 49, Springer, Berlin, 1981, p. 189.
[36] M.H. Crozier, W.A. Runciman, J. Chem. Phys. 35 (1961) 1392.
[37] P. Dorenbos, J. Andriessen, C.W.E. van Eijk, J. Solid State Chem. 171 (2003) 133.
[38] L. Pauling, The Nature of Chemical Bond, third ed., Cornell University Press, New York, 1960.
[39] K. Pátek, Glass Lasers, Butterworth, London, 1970.
[40] N. Rakov, G.S. Maciel, C.B. Araújo, Y. Messaddeq, J. Appl. Phys. 91 (2002) 1272.
[41] T. Kishimoto, N. Wada, K. Kojima, Phys. Chem. Glasses 43 (2002) 233.
[42] K. Soga, H. Inoue, A. Makishima, S. Inoue, J. Lumin. 55 (1993) 17.
[43] S. Todoroki, S. Tanabe, K. Hirao, N. Soga, J. Non-Cryst. Solids 136 (1991) 213.
[44] R. Cases, M.A. Chamarro, J. Solid State Chem. 90 (1991) 313.
[45] S. Tanabe, S. Yoshii, K. Hirao, N. Soga, Phys. Rev. B 45 (1992) 4620.
[46] R.D. Shannon, C.T. Prewitt, Acta Cryst. 26 (1970) 1046.